# NEW INSIGHTS INTO CALLISTO'S SURFACE COMPOSITION WITH THE GROUND-BASED NEAR-INFRARED IMAGING SPECTROMETER SINFONI OF THE VLT.

**N. Ligier[1], W.M. Calvin[2], J. Carter[3], F. Poulet[3], C. Paranicas[4], C. Snodgrass[5]**

*[1]School of Physical Sciences, The Open University, Milton Keynes MK7 6AA, UK. [2]Geological Sciences & Engineering, University of Nevada, Reno NV 89557, USA. [3]Université Paris-Saclay, CNRS, Institut d'Astrophysique Spatiale, 91405 Orsay, France. [4]Applied Physics Laboratory, Johns Hopkins University, Laurel MD 20723, USA. [5]School of Physics and Astronomy, University of Edinburgh, Edinburgh EH8 9YL, UK.*

***First author contact: nicolas.ligier@open.ac.uk***

**Context:** Callisto, the outermost of the four Galilean satellites, has arguably received the least research attention among the four moons. However, like Europa and Ganymede, Callisto also likely possesses a sub-glacial ocean, which is trapped between two layers of ice and is potentially habitable [**1**]. During the 2020s, ESA's mission JUICE will investigate the surface composition of the moon, getting data with a spatial resolution down to a few hundred meters or less through dozens of fly-bys. The imaging spectrometer MAJIS, operating from the visible (0.5 µm) to the mid infrared (5.54 µm), aims to detect and characterize the properties of the different species existing on Callisto's surface [**2**]. In preparation for the mission and the instrument, ground-based observations were performed of the three icy Galilean satellites. Callisto was observed during four nights with the near-infrared integral field spectrometer SINFONI of the VLT. In this abstract we describe the results of the properties and composition of Callisto's surface derived from 4 nights of observation.

**Instrument:** SINFONI combines one adaptive optics module and an integral field spectrometer operating with four gratings in the range 1.05 – 2.50 µm [**3**]. These observations were carried out using the widest grating, going from 1.40 to 2.50 µm, divided into 2200 spectral channels. Because SINFONI's FoV (0.8×0.8 arcsec) is divided into 64 × 64 pixels, each acquisition results in a 3D-cube (x, y, $\lambda$), with dimensions 64×64×2200. The very high spatial and spectral sampling of SINFONI, coupled with its great adaptive optics and its very high signal-to-noise ratio, allow to detect, characterize and map any features in Callisto's spectra.

**Dataset:** The first three observations were acquired in 2015, from January to March, and the last one was obtain in March 2016 (Table 1). In both cases, these periods corresponded to opposition with the Jovian system, thus providing the best angular resolution for the moon, about 1.5 arcsec in this case. Because SINFONI's FoV is about 0.8 arcsec, we had to acquire a mosaic of frames (10) to fully cover Callisto's disk. In addition, one of the main goals of this campaign was to cover Callisto's surface entirely. Hence, each observations aimed to investigate one phase of the moon. Some of the observational parameters useful for the data reduction are provided in Table 1.

| Acquisition date | Distance to Earth | Strehl ratio | SSP lat./long. |
|---|---|---|---|
| **2015/01/23** | 4.37 A.U. | 18.8 ± 1.2 | [158ºW, 0ºN] |
| **2015/02/16** | 4.37 A.U. | 27.1 ± 0.9 | [312ºW, 0ºN] |
| **2015/03/08** | 4.49 A.U. | 26.1 ± 1.0 | [20ºW, 0ºN] |
| **2016/03/19** | 4.44 A.U. | 28.8 ± 1.0 | [206ºW, -2ºN] |

***Table 1.*** *Main observational and geographical parameters of each observation. [1] SSP: Sub-Solar Point.*

**Data processing:** In order to get calibrated 3D-cubes of reflectance, numerous processing steps need to be performed. Most of the steps are described in a recently published paper about Ganymede [**4**]. Probably the most important is the photometric correction, which aims to remove effects due to the geometry of the observation. Our study shows that, like Ganymede, the Lambertian model is not sufficient to recover Callisto's surface reflectance, probably because of its roughness. Instead, the Oren-Nayar model, which generalizes the Lambertian model for rough surfaces [**5**], produces much better results and allows the recovery of reflectance up to inclination angles ~65° (Figure 1). The roughness parameter, named $\sigma$, is obtained empirically by iterating until 3D-cubes show no inclination residuals over the entire wavelength range. For Callisto, $\sigma$ ranges from 17° to 19°, similar values to those obtained for Ganymede with the same model [**4**]. No hemispherical variations are identified.

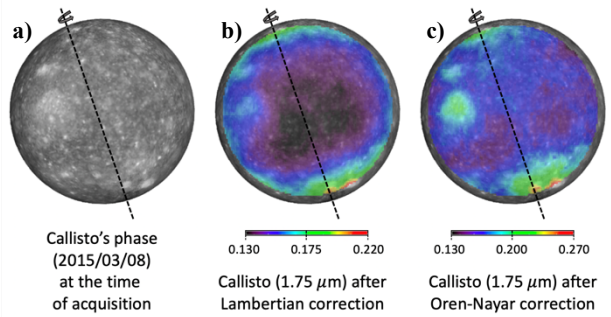


***Figure 1.*** *Results and differences between two photometric corrections for the 2015/03/08 observation: the Lambertian model (a) and the Oren-Nayar qualitative model (b).*

**Data modeling:** We use a linear unmixing approach to model the spectra. A non-linear, e.g. radiative transfer, approach is generally preferred but it requires optical con-

stants that are currently critically lacking at cryogenic temperatures for the non-ice species. After multiple tests, we found that Callisto's surface in SINFONI's H+K range is well modeled by using (1) a flat "greying" agent with a reflectance level varying from 0.12 to 0.22, (2) the crystalline ice with four different grain sizes (25 µm, 100 µm, 300 µm and 1 mm), and (3) a varying blue slope (Figure 2). The use of amorphous ice and any type of salty species does not improve our models at all, unlike Europa and Ganymede [**4**,**6**]. However, the greying agent is required to match the flatness of the spectra, as for those of Ganymede [**4**]. Hydrated silicates are suspected to be that unknown agent but this has not been uniquely identified due to the lack of detection of specific spectral signatures [**7**].

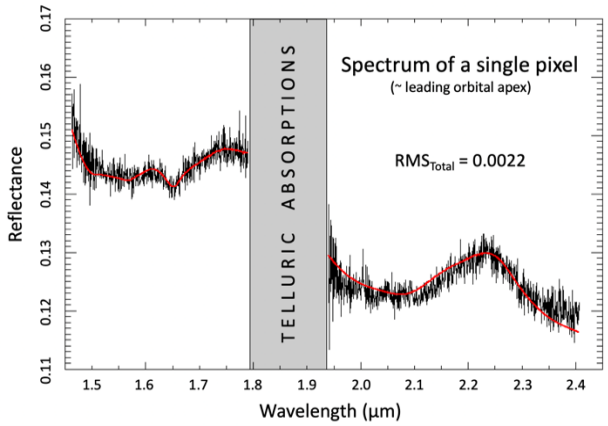


***Figure 2.*** *Spectral modeling (red) of a measured spectrum of a single pixel (black). The wavelength range 1.79 – 1.93 µm is not modeled because of strong telluric absorptions. In this case, the abundance of the greying agent reaches 92.8%, while the grains of crystalline ice are mostly 1 mm (4.5%) or 25 µm (2.3%) large.*

**Abundance maps and interpretations:** Global abundance maps of Callisto were obtained for each end-member used in the modeling. At large scale, the greying agent is by far the most abundant species over Callisto's surface (Figure 3a) with more than 90% of abundance overall. With the exception of some large craters and the latitudes beyond ±50°N, crystalline ice total abundance at all grain sizes rarely exceeds 10%. It is however important to mention that the relative content ice/non-icy material strongly depends on the type of mixture that is considered. The distribution of ice exhibits a light latitudinal gradient, especially the two smallest grain sizes (Figure 3b). The notable lack of water ice at the equator and the weak fall-off with latitude suggests sublimation by solar photons, in agreement with a former study [**8**]. At regional scale, spatial correlations are observed for some big impact craters, especially bright ones such as *Heimdall* and *Lofn*. At the same time, the large, and old, multi-ring impact crater *Valhalla* does not show similar enrichment in ice, suggesting that Callisto's surface has been progressively recovered by fine dusty particles since its formation. Finally, the map of the reflectance level for the greying agent exhibits an interesting spatial distribution (Figure 3c). This map shows clear and unexpected correlations, particularly with the two largest multi-ring impact craters of Callisto, *Asgard* and *Valhalla*; they both have a reflectance level quantitatively 0.03 higher than surrounding terrain. This variation could be explained by a different grain size or a different mixture for the greying agent. By the time of the meeting, additional analysis will be performed to further investigate the question.

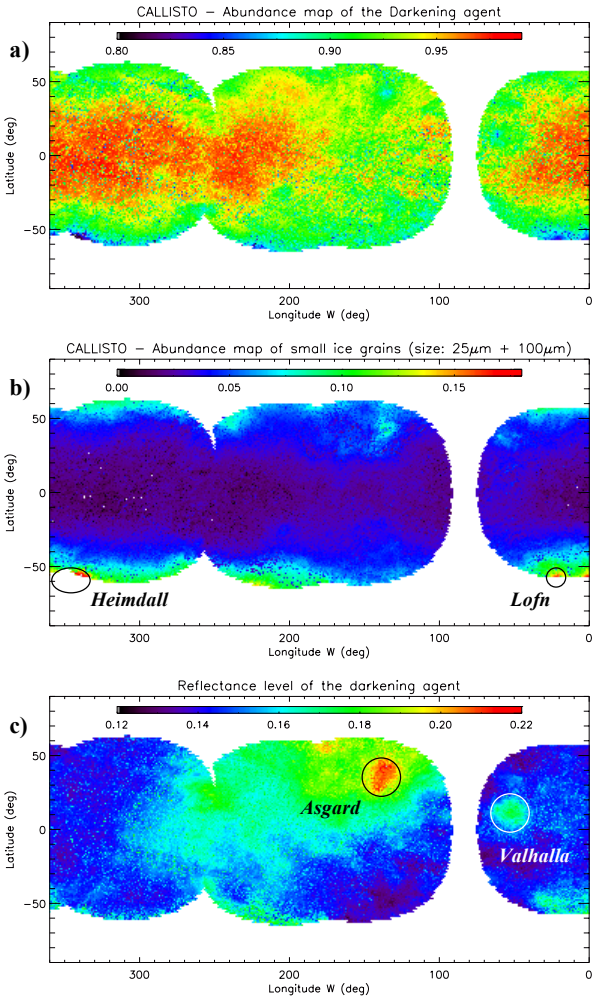


***Figure 3.*** *Maps obtained after global modeling: the abundance map of the grying agent (a), the abundance map of small grains of crystalline ice (b), and the map of the reflectance level used in the modeling for the greying agent (c).*

**References:** [**1**] Sotin & Tobie 2004, Comptes Rend. Phys. 5, 769 – 780. [**2**] Langevin et al. 2018, IPM, p. E1. [**3**] Eisenhauer et al. 2003, Proceedings of SPIE 4841, 1548 – 1561. [**4**] Ligier et al. 2019, Icarus 333, 496 – 515. [**5**] Oren & Nayar 1994, SIGGRAPH 94, ACM Press, 239 – 246. [**6**] Ligier et al. 2016, Astron. Journal 151, 163. [**7**] Calvin & Clark 1991, Icarus 89, 305 – 317. [**8**] Sieveka & Johnson 1982, Icarus 51, 528 – 548.